

# Influence of Soluble Oligomeric Aluminum on Precipitation in the Al-KOH-H<sub>2</sub>O System

Mateusz Dembowski<sup>a</sup>, Tren R Graham<sup>a</sup>, Jacob G. Reynolds<sup>b</sup>, Sue B. Clark<sup>a,c</sup>, Kevin M. Rosso<sup>a</sup>, and Carolyn I. Pearce<sup>a</sup>

<sup>a</sup>Pacific Northwest National Laboratory, Richland, Washington 99352, USA

<sup>b</sup>Washington River Protection Solutions, LLC, Richland, Washington 99352, USA

<sup>c</sup>Washington State University, Department of Chemistry, Pullman, WA 99164, USA

## Table of Contents

ICP-OES experimental details	pp. S2
Powder X-ray diffraction experimental details	pp. S2
Raman spectroscopy	pp. S3
Numerical analysis	pp. S4-6
Dimer-cation interactions	pp. S7
Powder X-ray diffraction results	pp. S8-12
<sup>27</sup> Al NMR	pp. S13
SEM micrographs	pp. S14

*Inductively coupled plasma optical emission spectrometry (ICP-OES)*

Concentration of solvated Al was determined on samples diluted in nitric acid (Optima trace metal grade, Fisher Scientific) with a Perkin Elmer Optima 2100 DV ICP-OES with an AS93 auto Sampler. Samples were introduced into the instrument via a Helix Tracey 4300 DV spray chamber and SeaSpray nebulizer at a flow rate of 1.5 mL/min. Indium and gallium were added to each sample as internal standards. Each sample was prepared in triplicate and reported values represent an average of measured values. The concentration of Al in each sample was determined from a calibration curve of standard solutions made with Ultra Scientific ICP standards (Kingstown, RI) in a range of 0.5 to 3000  $\mu\text{g/L}$ . Density of each solution was measured gravimetrically using a calibrated pipette and used to convert units from moles of aluminum per gram of solution to moles of aluminum per liter of solution.

*Powder X-ray diffraction (PXRD)*

Diffraction patterns were collected with a Phillips X'Pert Multi-Purpose diffractometer (PANalytical Almelo, The Netherlands) between 10 and 80 degrees two theta. The fixed Cu anode operated at 50 kV and 40 mA. Fitting of the resulting patterns was accomplished using JADE software (v. 9.5.1, Materials Data Inc.) in conjunction with the PDF4+ database (International Center for Diffraction Data). Only two solid phases have been observed in all analyzed solids corresponding to either  $\gamma\text{-Al(OH)}_3$  (ICDD ID: 04-011-1369), and/or  $\text{K}_2\text{Al}_2\text{O(OH)}_6$  (ICDD ID: 04-012-6223). The relative abundance of the two phases was determined using the refinement procedure as implemented in JADE software.

Raman spectroscopy

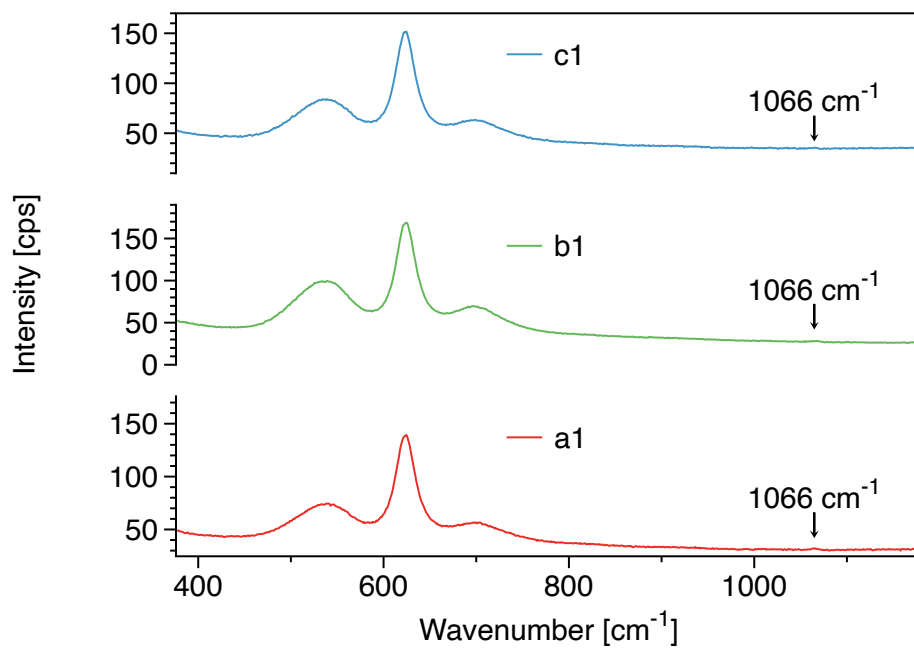


**Figure S1.** Raman spectra of solutions a1, b1, and c1 highlighting the signature associated with the carbonate anion,  $\text{CO}_3^{2-}$  at 1066  $\text{cm}^{-1}$ .

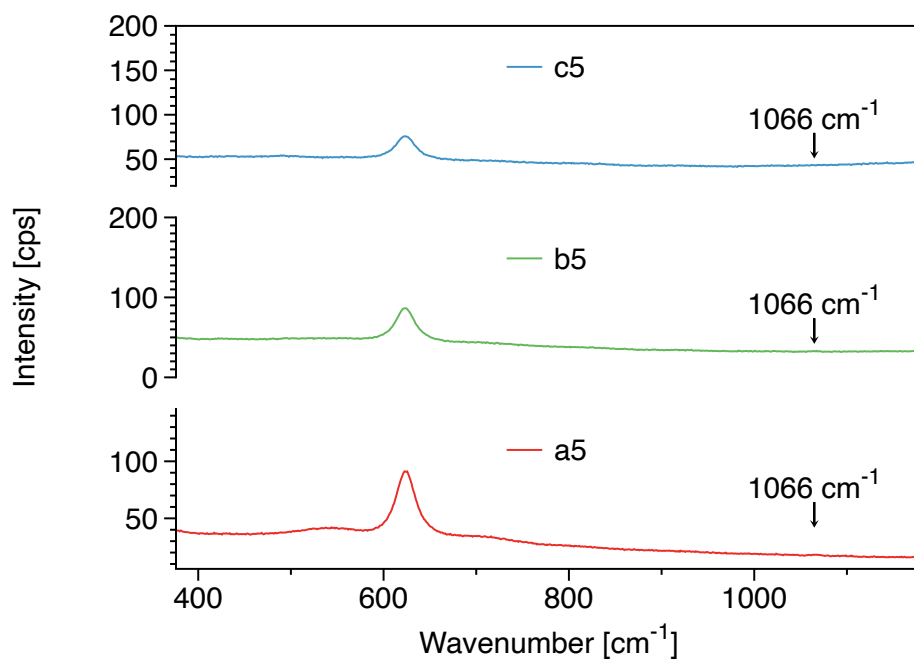


**Figure S2.** Raman spectra of solutions a5, b5, and c5 highlighting the signature associated with the carbonate anion,  $\text{CO}_3^{2-}$  at 1066  $\text{cm}^{-1}$ .

### Numerical analysis

Expression  $I_{698} = A \times I_{535} + B \times I_{623}$  has been proposed on basis of numerical analysis to account for variations in the  $I_{698}/I_{535}$  ratio observed in the aluminate systems.  $A$  and  $B$  are empirically determined constants and were originally reported as 0.38 and 0.08, respectively.

Numerical analysis was performed using *Solver* package as implemented in Microsoft® Excel for Mac (v. 16.40 20081000). Solver Parameters were set to minimize the SUM R<sup>2</sup> value, where R<sup>2</sup> was defined as the square of the difference in integrated signal intensity of the 700 peak and the calculated signal intensity of the 700 peak using the  $I_{698} = A \times I_{535} + B \times I_{623}$  expression, by varying the values of  $A$  and  $B$ . *GRG Nonlinear* solving method was utilized with forward derivatives and multistart option with a population size of 100. **Table S1** summarizes some of the  $A$  and  $B$  values determined in the present study

**Table S1.** Examples values of  $A$  and  $B$  obtained from numerical analysis

<b>Sample set</b>	<b>a1-5</b>	<b>b1-5</b>	<b>c1-5</b>	<b>all</b>
<i>A</i>	0.37	0.45	0.50	0.37
<i>B</i>	0.02	0.00	0.18	0.02

**Table S2.** Variations in the corrected  $I_{700}/I_{535}$  ratio as a function of empirical parameters A and B outlined in Table S1. Corrected  $I_{700}/I_{535}$  ratio is based on use of A and B parameters for individual sample sets.

<b>Sample</b>	<b>Area 535 measured</b>	<b>Area 623 measured</b>	<b>Area 700 measured</b>	<b>Area 700 calculated</b>	<b>2<sup>nd</sup> harmonic contribution</b>	<b>Area 700 corrected</b>	<b><math>I_{700}/I_{535}</math> corrected</b>
<b>a1</b>	2675	2146	4069	1060	65.95	2079.65	0.78
<b>a2</b>	1320	1111	3162	542	51.24	1059.46	0.80
<b>a3</b>	742	393	2107	310	34.16	359.12	0.48
<b>a4</b>	405	174	1458	174	23.63	150.44	0.37
<b>a5</b>	172	81	1080	81	17.50	63.80	0.37
<b>b1</b>	4052	3035	4849	1828	0.00	3035.10	0.75
<b>b2</b>	2427	2078	4474	1095	0.00	2078.30	0.86
<b>b3</b>	1054	1027	3233	475	0.00	1027.40	0.97
<b>b4</b>	757	449	2289	342	0.00	448.71	0.59
<b>b5</b>	418	189	1737	189	0.00	188.76	0.45
<b>c1</b>	2213	1793	3742	1783	672.04	1120.96	0.51
<b>c2</b>	2891	2273	4309	2225	773.86	1499.54	0.52
<b>c3</b>	2193	1923	4581	1923	822.65	1100.75	0.50
<b>c4</b>	1029	1147	3205	1092	575.47	571.63	0.56
<b>c5</b>	517	694	2419	694	434.43	259.74	0.50

Where 'Area 700 calculated' utilized the  $I_{698} = A \times I_{535} + B \times I_{623}$  expression together with specific values of A and B, '2<sup>nd</sup> harmonic contribution' = 'Area 700 measured' - (B x I<sub>623</sub>), 'Area 700 corrected' = 'Area 700 measured' - '2<sup>nd</sup> harmonic contribution', and ' $I_{700}/I_{535}$  corrected' = 'Area 700 corrected'/'Area 535 measured'.

**Table S3.** Variations in the corrected  $I_{700}/I_{535}$  ratio as a function of empirical parameters A and B outlined in Table S1. Corrected  $I_{700}/I_{535}$  ratio is based on use of A and B parameters for c1-5.

<b>Sample</b>	<b>Area 535 measured</b>	<b>Area 623 measured</b>	<b>Area 700 measured</b>	<b>Area 700 calculated</b>	<b>2<sup>nd</sup> harmonic contribution</b>	<b>Area 700 corrected</b>	<b><math>I_{700}/I_{535}</math> corrected</b>
<b>a1</b>	2675	2146	4069	2073	730.69	1414.91	0.53
<b>a2</b>	1320	1111	3162	1230	567.73	542.97	0.41
<b>a3</b>	742	393	2107	751	378.42	14.86	0.02
<b>a4</b>	405	174	1458	465	261.80	-87.73	-0.22
<b>a5</b>	172	81	1080	280	193.89	-112.59	-0.66
<b>b1</b>	4052	3035	4849	2905	870.82	2164.28	0.53
<b>b2</b>	2427	2078	4474	2022	803.37	1274.93	0.53
<b>b3</b>	1054	1027	3233	1110	580.59	446.81	0.42
<b>b4</b>	757	449	2289	791	411.01	37.70	0.05
<b>b5</b>	418	189	1737	522	311.92	-123.16	-0.29
<b>c1</b>	2213	1793	3742	1783	672.04	1120.96	0.51
<b>c2</b>	2891	2273	4309	2225	773.86	1499.54	0.52
<b>c3</b>	2193	1923	4581	1923	822.65	1100.75	0.50
<b>c4</b>	1029	1147	3205	1092	575.47	571.63	0.56
<b>c5</b>	517	694	2419	694	434.43	259.74	0.50

**Table S4.** Variations in the corrected  $I_{700}/I_{535}$  ratio as a function of empirical parameters  $A$  and  $B$  outlined in Table S1. Corrected  $I_{700}/I_{535}$  ratio is based on use of  $A$  and  $B$  parameters for all sample sets.

<b>Sample</b>	<b>Area 535 measured</b>	<b>Area 623 measured</b>	<b>Area 700 measured</b>	<b>Area 700 calculated</b>	<b>2<sup>nd</sup> harmonic contribution</b>	<b>Area 700 corrected</b>	<b><math>I_{700}/I_{535}</math> corrected</b>
<b>a1</b>	1320	1111	3162	542	65.95	2079.65	0.78
<b>a2</b>	742	393	2107	310	51.24	1059.46	0.80
<b>a3</b>	405	174	1458	174	34.16	359.12	0.48
<b>a4</b>	172	81	1080	81	23.63	150.44	0.37
<b>a5</b>	4052	3035	4849	1585	17.50	63.80	0.37
<b>b1</b>	2427	2078	4474	975	78.60	2956.50	0.73
<b>b2</b>	1054	1027	3233	444	72.51	2005.79	0.83
<b>b3</b>	757	449	2289	319	52.40	975.00	0.92
<b>b4</b>	418	189	1737	184	37.10	411.61	0.54
<b>b5</b>	2213	1793	3742	883	28.15	160.61	0.38
<b>c1</b>	2891	2273	4309	1145	60.66	1732.34	0.78
<b>c2</b>	2193	1923	4581	889	69.85	2203.55	0.76
<b>c3</b>	1029	1147	3205	435	74.25	1849.15	0.84
<b>c4</b>	517	694	2419	232	51.94	1095.16	1.06
<b>c5</b>	1320	1111	3162	542	39.21	654.96	1.27

**Table S5.** Variations in the corrected  $I_{700}/I_{535}$  ratio as a function of empirical parameters  $A$  and  $B$  reported in the original study.  $A = 0.38$ ,  $B = 0.08$

<b>Sample</b>	<b>Area 535 measured</b>	<b>Area 623 measured</b>	<b>Area 700 measured</b>	<b>Area 700 calculated</b>	<b>2<sup>nd</sup> harmonic contribution</b>	<b>Area 700 corrected</b>	<b><math>I_{700}/I_{535}</math> corrected</b>
<b>a1</b>	1320	1111	3162	1342	325.52	1820.08	0.68
<b>a2</b>	742	393	2107	755	252.92	857.78	0.65
<b>a3</b>	405	174	1458	450	168.58	224.70	0.30
<b>a4</b>	172	81	1080	270	116.63	57.44	0.14
<b>a5</b>	4052	3035	4849	152	86.38	-5.08	-0.03
<b>b1</b>	2427	2078	4474	1928	387.94	2647.16	0.65
<b>b2</b>	1054	1027	3233	1280	357.90	1720.40	0.71
<b>b3</b>	757	449	2289	659	258.65	768.75	0.73
<b>b4</b>	418	189	1737	471	183.10	265.61	0.35
<b>b5</b>	2213	1793	3742	298	138.96	49.80	0.12
<b>c1</b>	2891	2273	4309	1140	299.39	1493.61	0.67
<b>c2</b>	2193	1923	4581	1443	344.75	1928.65	0.67
<b>c3</b>	1029	1147	3205	1200	366.49	1556.91	0.71
<b>c4</b>	517	694	2419	647	256.37	890.73	0.87
<b>c5</b>	1320	1111	3162	390	193.54	500.63	0.97

*Dimer-cation interactions*

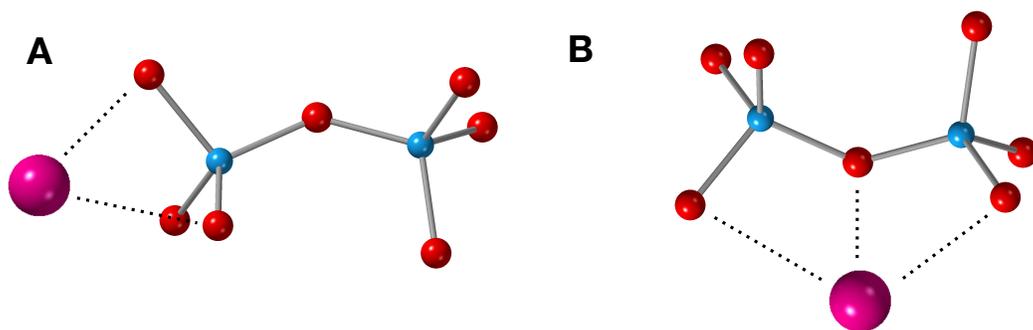


**Figure S3.** Examples of possible contact ion pair (CIP) configurations between  $\text{Al}_2\text{O}(\text{OH})_6^{2-}$  and  $\text{K}^+$ . CIPs occurring via (left) the terminal  $\text{Al}(\text{OH})_3$  unit and (right) the bridging  $\mu\text{-O}$  atom. Blue, magenta, and red spheres represent aluminum, potassium, and oxygen atoms respectively.

## Powder X-ray Diffraction Results

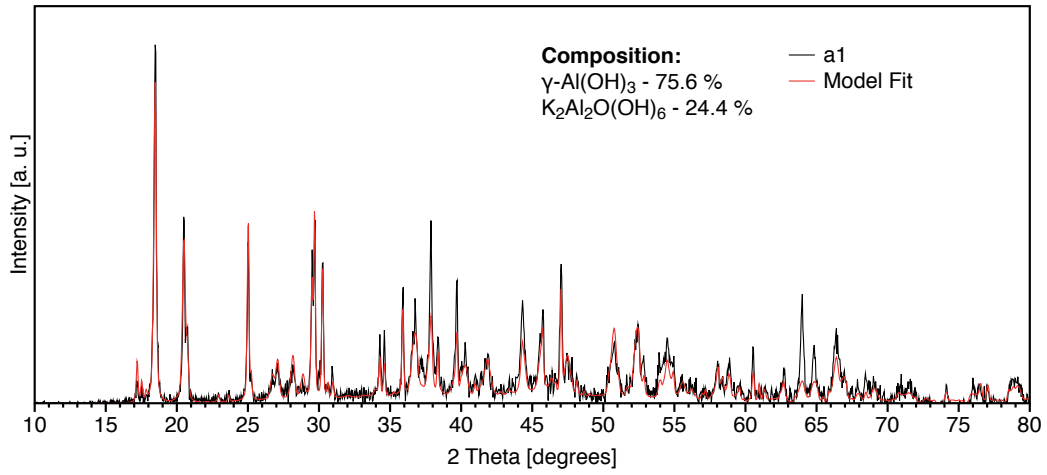


Figure S4. PXRD pattern of solid retrieved from reaction a1.

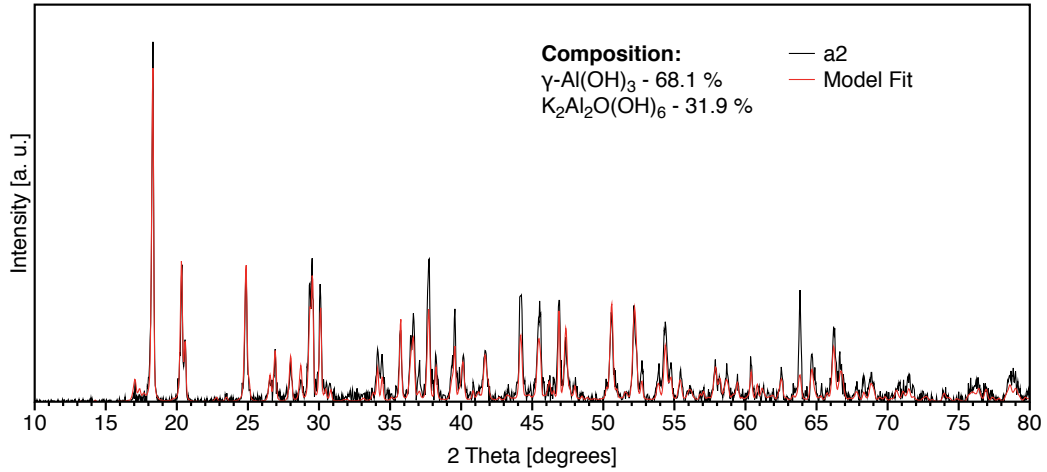


Figure S5. PXRD pattern of solid retrieved from reaction a2.

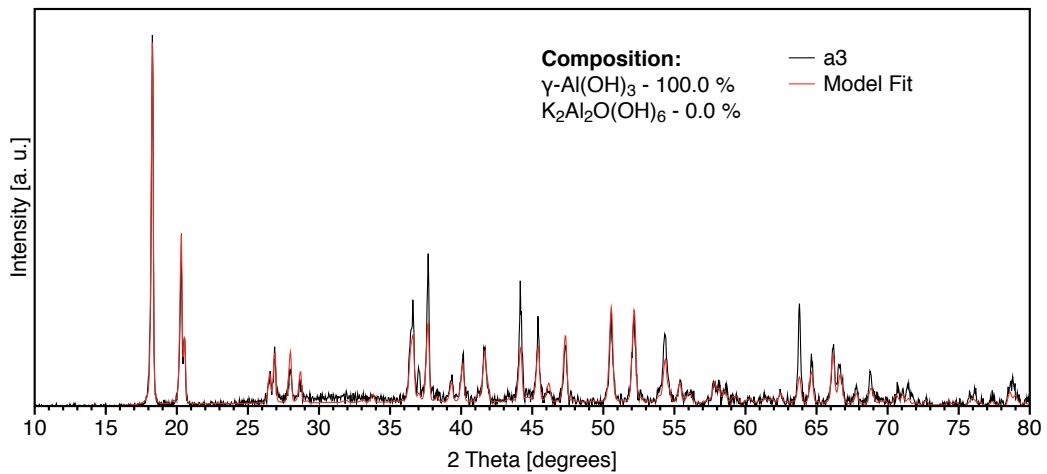
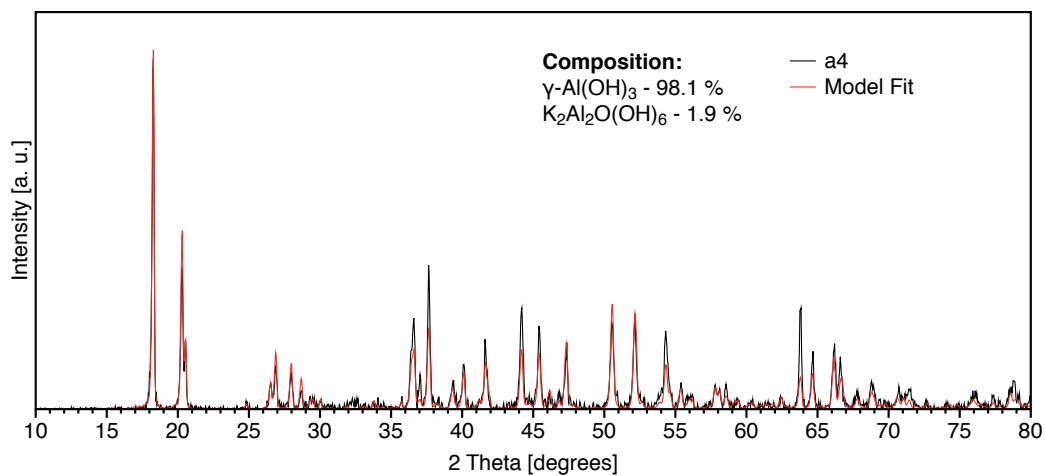
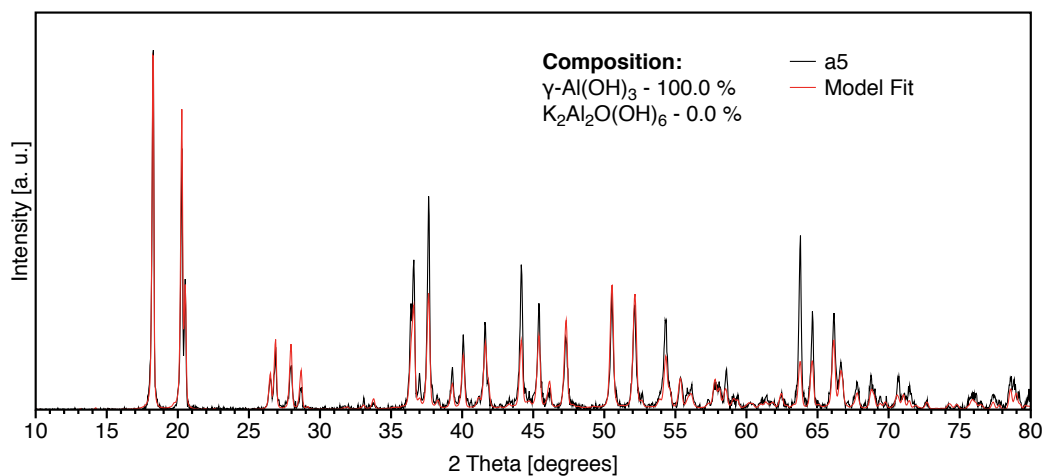


Figure S6. PXRD pattern of solid retrieved from reaction a3.



**Figure S7.** PXRD pattern of solid retrieved from reaction a4.



**Figure S8.** PXRD pattern of solid retrieved from reaction a5.

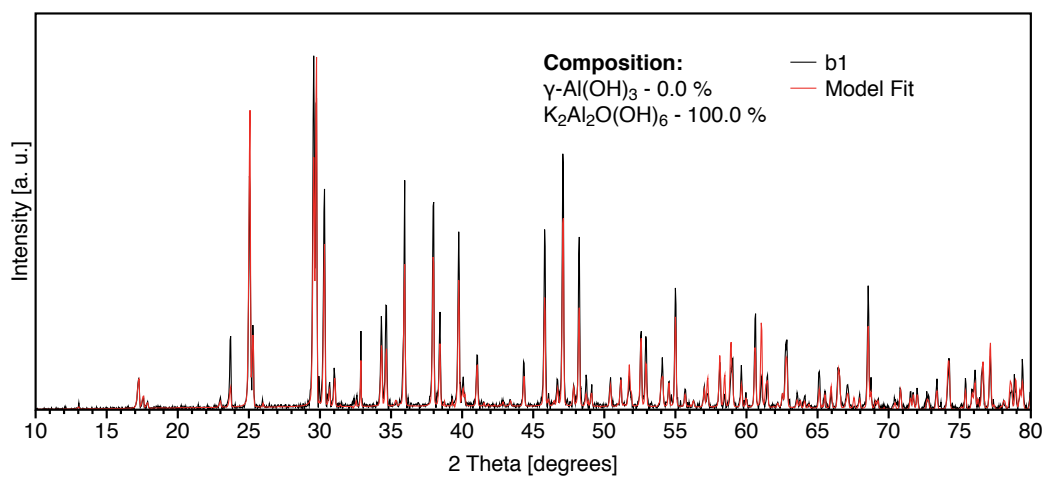


**Figure S9.** PXRD pattern of solid retrieved from reaction b1.

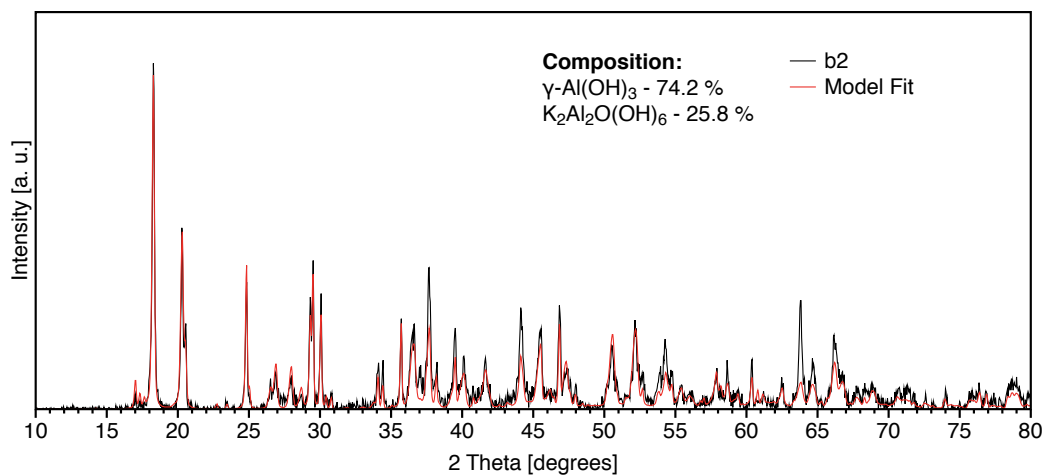


**Figure S10.** PXRD pattern of solid retrieved from reaction b2.

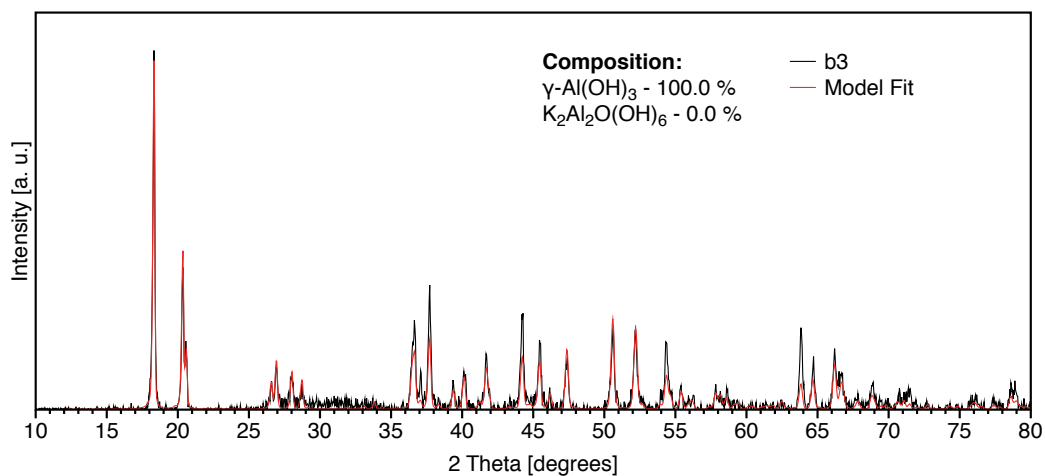


**Figure S11.** PXRD pattern of solid retrieved from reaction b3.

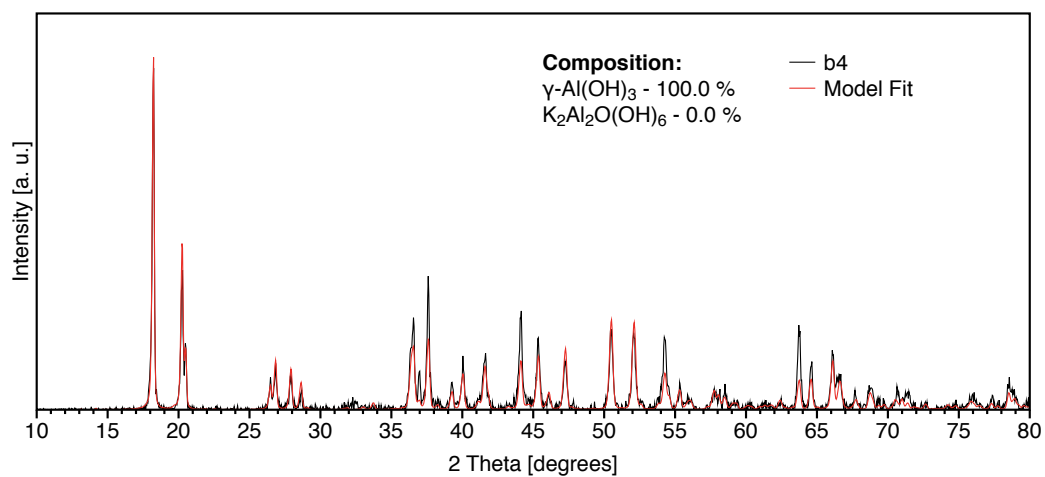


**Figure S12.** PXRD pattern of solid retrieved from reaction b4.

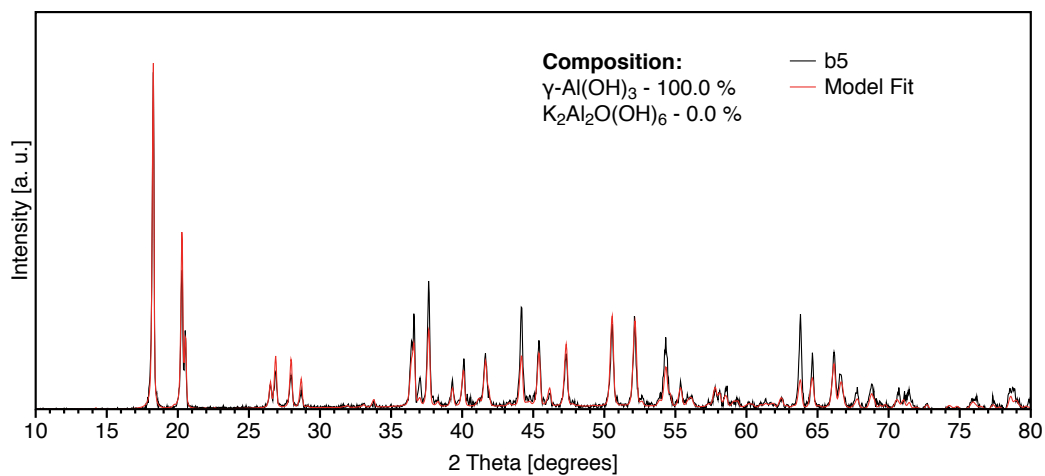


**Figure S13.** PXRD pattern of solid retrieved from reaction b5.

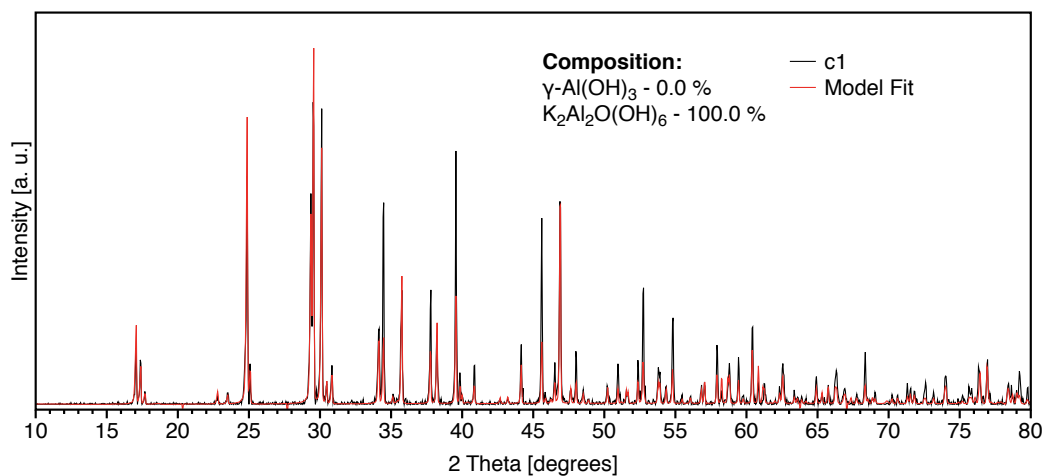


**Figure S14.** PXRD pattern of solid retrieved from reaction c1.

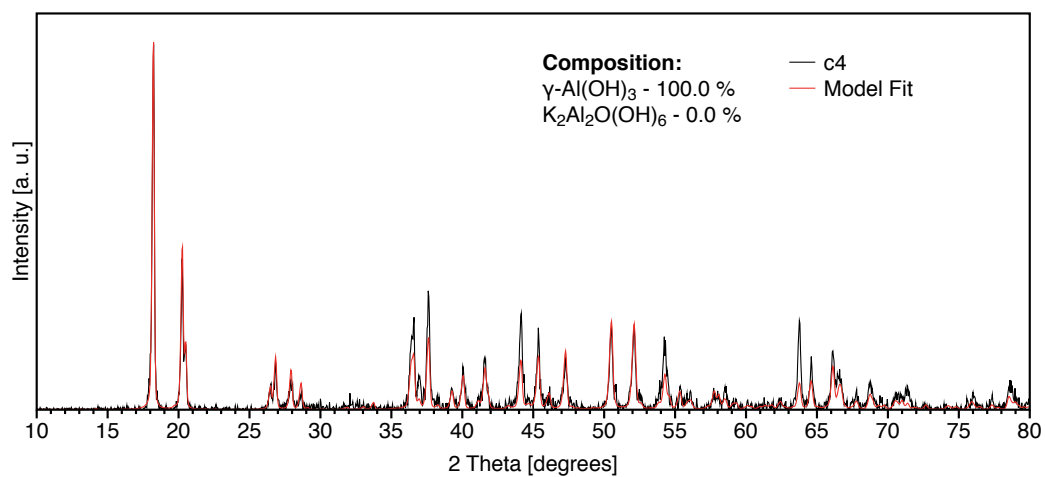


**Figure S15.** PXRD pattern of solid retrieved from reaction c4.

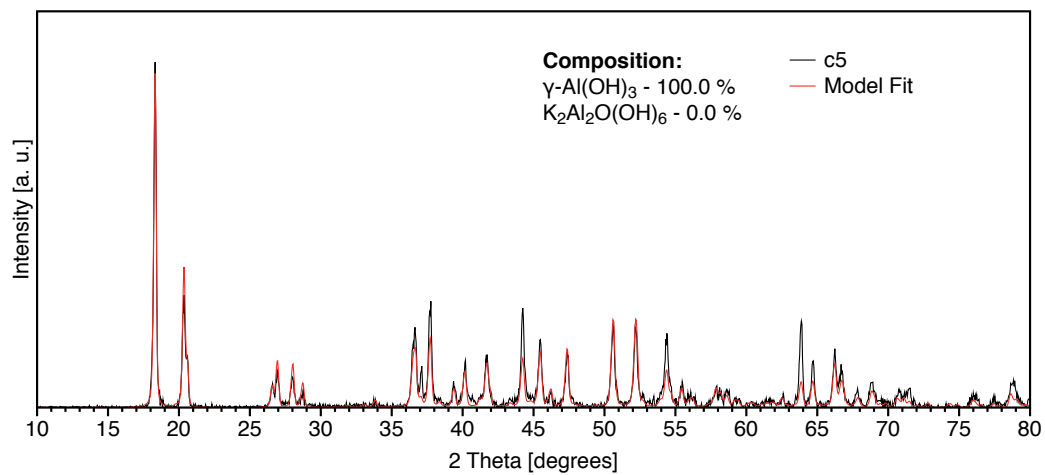


**Figure S16.** PXRD pattern of solid retrieved from reaction c5.

## <sup>27</sup>Al NMR results

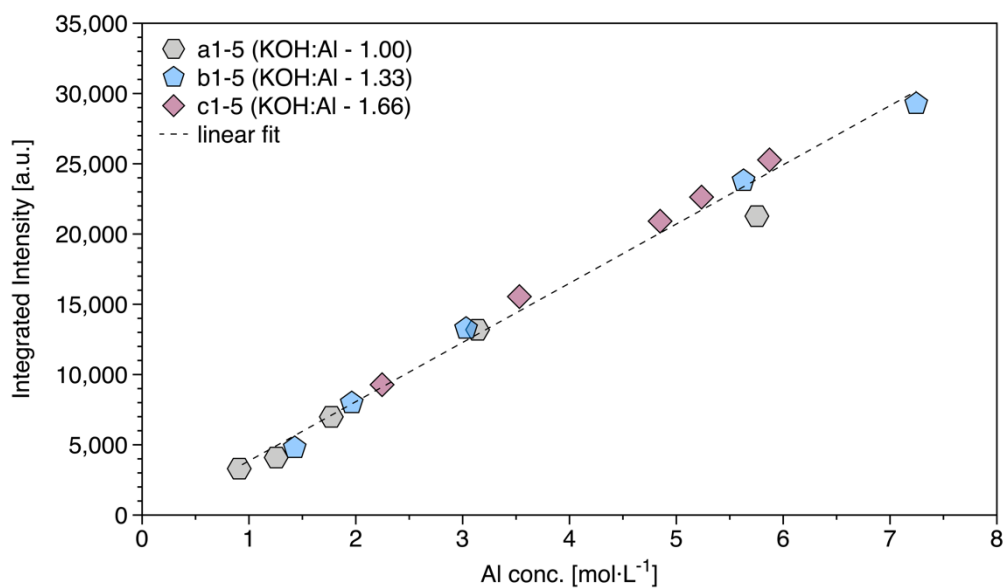


**Figure S17.** Correlation between the integrated intensity of aluminate signals in <sup>27</sup>Al NMR and the concentration of Al in solution determined via ICP-OES.

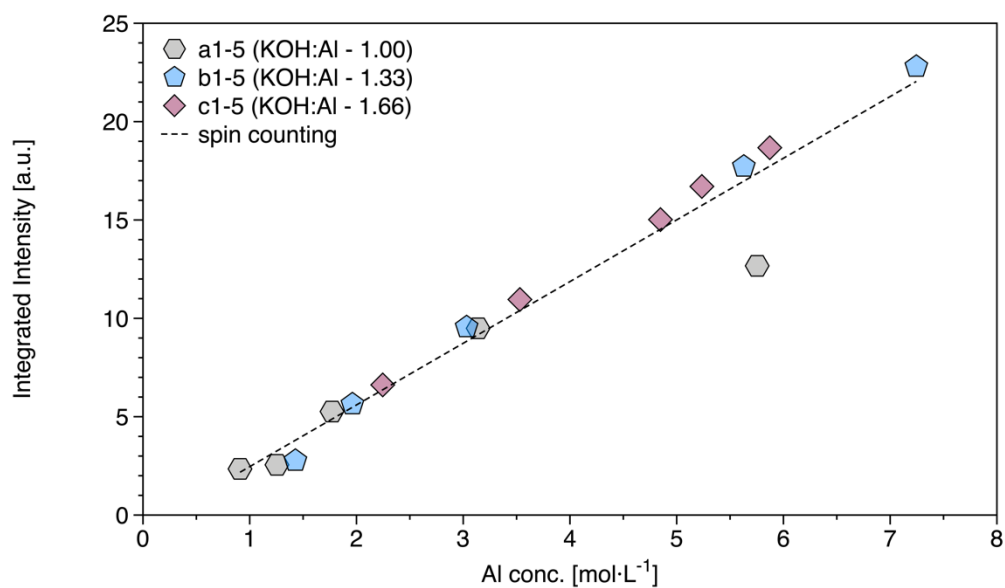


**Figure S18.** Correlation between the normalized integrated intensity of aluminate signals in <sup>27</sup>Al NMR and the concentration of Al in solution determined via ICP-OES.

SEM micrographs

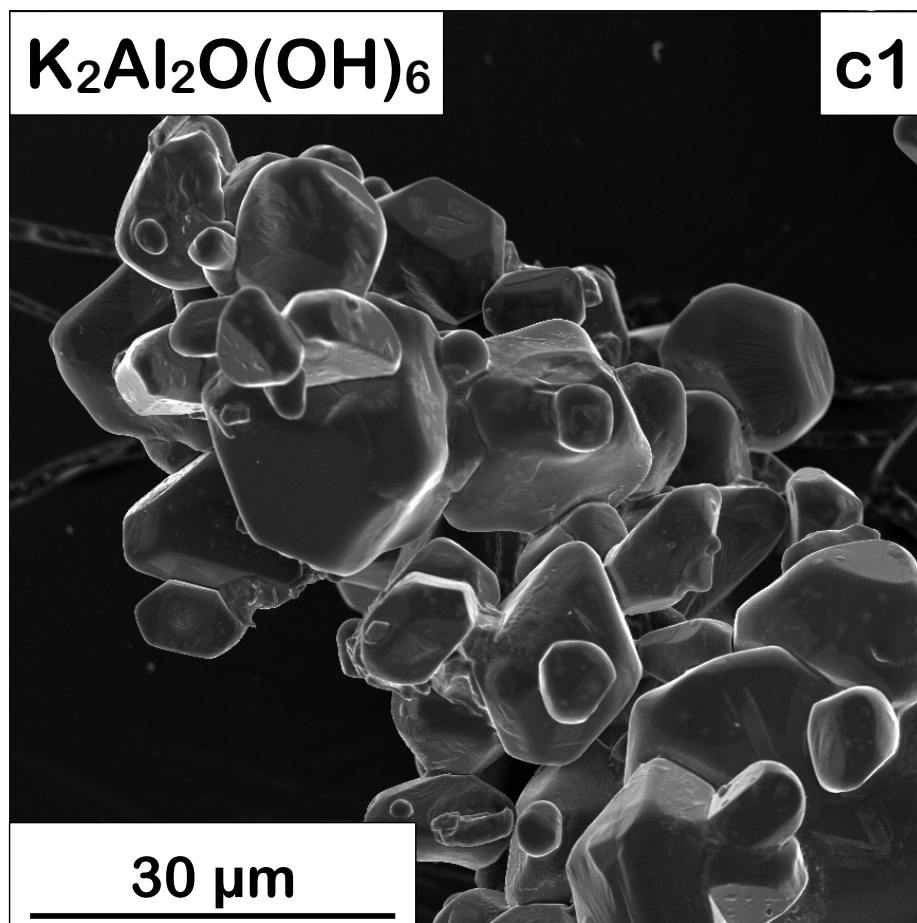


Figure S19. SEM micrograph of the pure  $K_2Al_2O(OH)_6$  phase retrieved from experiment c1.